

Spring Technical Meeting  
Eastern States Section of the Combustion Institute  
March 6-9, 2022  
Orlando, Florida

# Premixed Laminar Oxycombustion of Hydrogen with Carbon Dioxide as a Working Fluid

*Md Nayer Nasim<sup>1,\*</sup>, Behlol Nawaz<sup>1</sup>, Amina SubLaban<sup>1</sup>, and J. Hunter Mack<sup>1</sup>*

*<sup>1</sup>Department of Mechanical Engineering, University of Massachusetts Lowell,  
1 University Avenue, MA, USA*

\*Corresponding Author Email: mdnayer\_nasim@student.uml.edu

**Abstract:** Hydrogen ( $H_2$ ) is an attractive alternative fuel due to its inherent carbon-free emissions and potential compatibility with the existing transportation and energy conversion technologies. However, outside of generation/distribution concerns, several challenges exist before widespread implementation - including fundamentally different combustion properties in comparison to natural gas and other common hydrocarbon fuels. For example, the maximum laminar burning velocity (LBV) of hydrogen is over 7 times greater than that of natural gas when combusted in air, where nitrogen is the primary working fluid. To balance this dramatic increase, carbon dioxide ( $CO_2$ ) can be used as a working fluid to reduce the speed with which a flame front expands. The combination of hydrogen as a fuel with carbon dioxide as a working fluid therefore provides the opportunity to achieve flames with LBVs that are appropriate for practical combustion applications such as internal combustion engines and gas turbines. Furthermore, the inclusion of  $CO_2$  avoids the production of  $NO_x$  emissions and enables several opportunities for carbon sequestration or closed-cycle processes. This study experimentally explores the premixed oxycombustion properties of  $H_2/CO_2$  mixtures in a constant volume combustion chamber (CVCC) at varied initial pressures and equivalence ratios. The spherically expanding flames are examined to determine the laminar burning velocity, flammability limits, and instabilities present in the  $H_2/O_2/CO_2$  system.

**Keywords:** *Hydrogen, Carbon Dioxide, Premixed Combustion, Laminar Burning Velocity, Z-type Schlieren Technique.*

## 1. Introduction

The challenges facing conventional fossil fuels, such as limited reserves [1], their role in climate change [2], and harmful emissions [3], have accelerated interest in alternatives. Hydrogen is a promising candidate, as it has the potential to be generated using renewable sources [4] and produce significantly less harmful products [5]. While hydrogen could be compatible with the transportation and conversion technologies for other gaseous fuels, it is not the default case as the combustion of hydrogen is fundamentally different compared to the conventional fuels. This makes direct replacement with hydrogen difficult for internal combustion engines [5-6] and gas turbines [7].

The combustion of a fuel mixture can be characterized using several parameters. Flame speed, flame structure, and shape are all important, as they influence the rates of fuel consumption and energy release. Another very important characteristic is the laminar burning velocity (LBV), which indirectly helps in understanding a fuel mixture's reactivity, diffusivity, and exothermic behavior. It has been used in turbulent combustion models, chemical kinetic mechanism development, and the design/optimization of engines. The combustion of hydrogen is more energetic compared to  $CH_4$  and this manifests as a LBV seven times higher with nitrogen as the working fluid. This has consequences for the operation and safety of any technology that uses hydrogen combustion. It could be significantly easier, cost effective, and safer if the combustion of hydrogen can be modified to resemble methane ( $CH_4$ ) or natural gas. Carbon dioxide ( $CO_2$ ) reduces the speed with which the flame front expands [8]. Combining  $CO_2$  as a working fluid with hydrogen as a fuel can therefore provide a balance to the inherently high LBV. The use of  $CO_2$  instead of nitrogen also has the added benefit of eliminating the potential for  $NO_x$  emissions. Furthermore, it can be used to work in conjunction with carbon sequestration and closed-cycle processes. It is therefore worth

investigating the effect of CO<sub>2</sub> as a working fluid with hydrogen for potential applications. Similar studies for other mixtures containing hydrogen and methane exist [9-10], but the existing literature lacks in the specific variables and the combustion properties considered here for H<sub>2</sub>/O<sub>2</sub>/CO<sub>2</sub> mixtures.

This study investigates the effects of changing equivalence ratios ( $\phi = 0.6, 0.8, \text{ and } 1.0$ ) under numerous initial pressures ( $P_i = 1.0, 1.5, \text{ and } 2.0$  bar), with varying fractions of CO<sub>2</sub> (20%, 40%, and 60%) as the working fluid. This is carried out in an optically accessible constant volume combustion chamber (CVCC) using a Z-type Schlieren imaging setup in conjunction with pressure measurements. The flame speed, laminar burning velocity, flame morphology, and Markstein length are studied using the high-speed images and pressure measurements for all initial conditions.

## 2. Methodology

### 2.1 Experimental Setup

A constant volume combustion chamber (CVCC) is used in combination with a Schlieren imaging setup to record the expanding flame with a highspeed camera. The experimental setup and procedure used in these experiments are described in a previous publication [11]. The chamber and gas supply lines are vacuumed down to 300 millitorrs before any gases are added to the system. The gases (H<sub>2</sub>, O<sub>2</sub>, and CO<sub>2</sub>) are always loaded into the chamber in ascending order of partial pressure. The amount of each gas added is determined by a matrix composed of partial pressure for each gas based off CO<sub>2</sub>%, equivalence ratio ( $\phi$ ), and initial pressure. Each initial condition is repeated three times to ensure a >95% confidence level.

### 2.2 Flame Speed

The images recorded during flame propagation are digitally processed to determine the flame speed, using Eq. 1, where  $dr_f$  is the change of flame radius (cm) and  $dt$  is the change in time (s):

$$S_b = \frac{dr_f}{dt} \quad (1)$$

The flame fronts in the images are used to calculate flame radii and consequently flame speed. Only the flame radii between 14 mm and 40 mm are considered, with the lower limit set to nearly 10 times the 1.36 mm distance between electrodes. The flame radii's upper limit of 40 mm was set to include flame edge data points prior to any physical contact with the chamber walls or any protruding instruments.

### 2.2 Laminar Burning Velocity

The laminar burning velocity is calculated with a constant volume combustion approach, which employs a thermodynamic multi-shell model (chamber is divided into two regions, burned and unburned gases, separated by the flame front and another thermal boundary between the unburned gas and the wall of the chamber) using experimental pressure data as the input. The model considers conservation of mass, conservation of energy, and ideal gas laws when treating the gas mixture and flame propagation system. Equation 2 represents the calculated laminar burning velocities which are fit to power law correlations using the least square method where  $S_u$  (m/s),  $T_u$  (K), and  $P$  (MPa) stand for the laminar burning velocity, unburned gas temperature and pressure of gas mixture, respectively [12]. Variables with 0 sub-indices refer to the values found at 298 K and 1 bar.

$$S_u = S_{u_0} \left\{ 1 + \beta \log \left( \frac{P}{P_0} \right) \right\} \left( \frac{T_u}{T_{u_0}} \right)^\alpha \quad (2)$$

$$S_{u_0} = 2.98 - 1.00(\phi - 1.70)^2 + 0.32(\phi - 1.70)^3 \quad (3)$$

The  $\alpha$  and  $\beta$  values are calculated using Equations 4 and 5

$$\alpha = 1.54 + 0.026 (\phi - 1) \quad (4)$$

$$\beta = 0.43 + 0.003 (\phi - 1) \quad (5)$$

Lastly, the constants in Equation 2 are calculated based on the least squares method and are recorded in Table 1. The fundamentals of the model, developed by Metghalchi and Keck, are elaborated on in past literature [13] and the complete mathematical details of the conversion of pressure data to laminar burning velocity are outlined in a previous publication [11].

**Table 1:** The constants used in Equation (2) for hydrogen-oxygen-carbon dioxide mixtures

	$\alpha$	$\beta$
$\phi = 1$	1.54	0.43
$\phi = 0.8$	1.53	0.42
$\phi = 0.6$	1.52	0.42

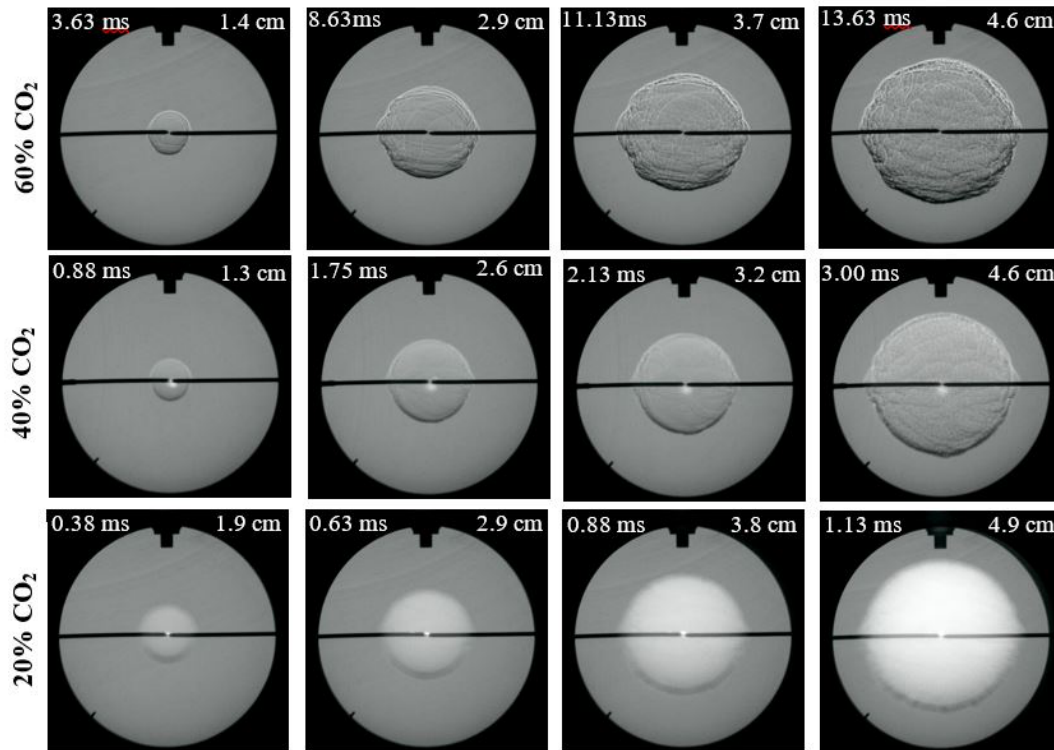


**Figure 1:** Schlieren images of H<sub>2</sub>-O<sub>2</sub>-CO<sub>2</sub> flame fronts at  $\phi = 1$  and  $P_i = 1$  bar

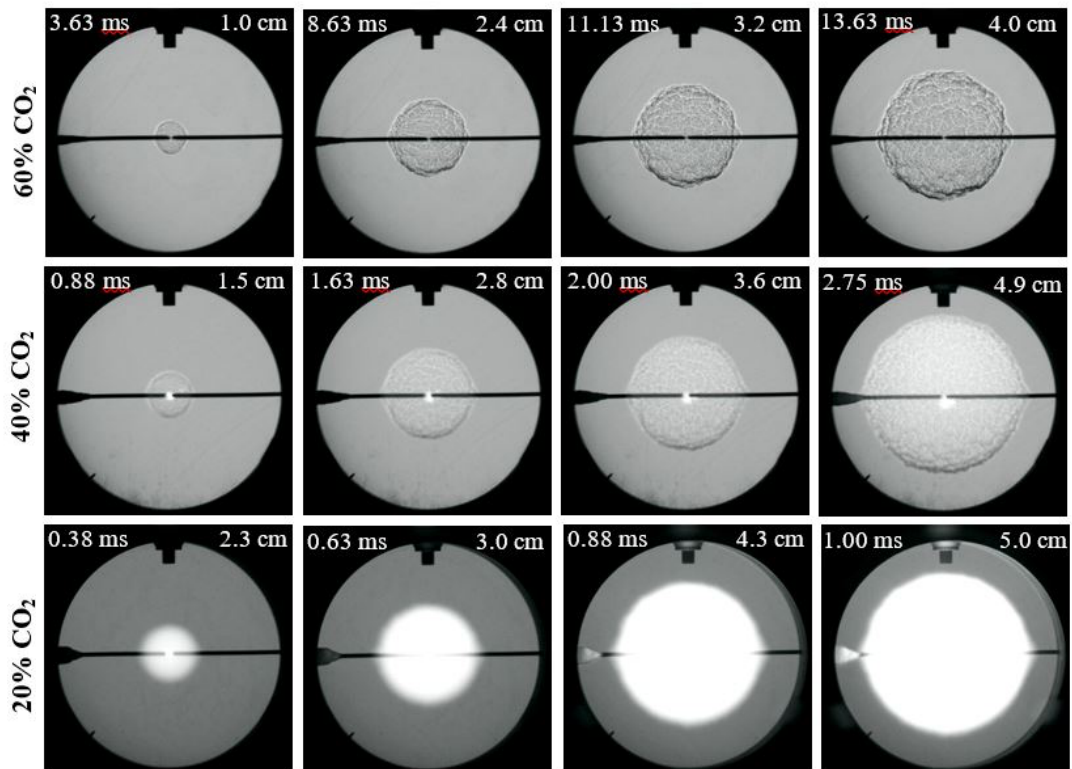


**Figure 2:** Schlieren images of H<sub>2</sub>-O<sub>2</sub>-CO<sub>2</sub> flame fronts at  $\phi = 1$  and  $P_i = 2$  bar

### 3. Results and Discussion

#### 3.1 Flame Morphology

Figures 1 and 2 present the Schlieren images of the spherically expanding flames inside the CVCC for H<sub>2</sub>-O<sub>2</sub>-CO<sub>2</sub> combustion at stoichiometric conditions and different initial pressures and fractions of CO<sub>2</sub>. The flame front propagates the fastest when the mixture contains 20% CO<sub>2</sub>. The flame speed decreases as the percentage of CO<sub>2</sub> increases. At both 20% and 40% CO<sub>2</sub> conditions, the flame front propagates faster as the initial pressure is increased from standard pressure to an elevated pressure (2 bar). A similar trend was observed by Ijima and Takeno [12] for hydrogen-air combustions. However, as the percentage of CO<sub>2</sub> was increased in the mixture, this trend changed, and the flame speed started to decrease with increasing initial pressures. At this stage, the hydrogen oxycombustion started showing characteristics like that of natural gas combustion, where the flame speed decreases with increasing initial pressures [11]. This can be attributed to the high thermal heat capacity of CO<sub>2</sub> compared to N<sub>2</sub> (~35 times) where it acts like a heat sink and decreases the net reaction rate, thereby reducing flame speed. Increasing the CO<sub>2</sub> concentration of the mixture, lowers the ability to overcome the activation energy for reactions to occur [8].

#### 3.2 Flame Speed

The correlation between the flame speed and the stretch rate at different initial pressures and different equivalence ratios has been explored to characterize the flame front. The concentration of CO<sub>2</sub> in these cases was 20%, 40%, or 60%. Due to the extremely high flame speed of 20% CO<sub>2</sub> mixture, the focus of this study will be on CO<sub>2</sub> concentrations of 40% and 60%.

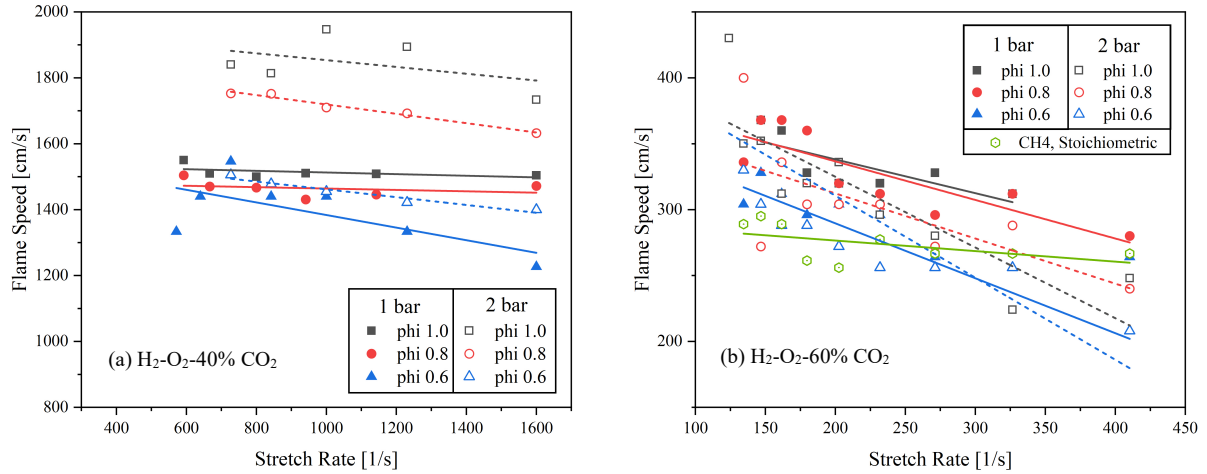


**Figure 3:** Variation of the flame speed ( $S_b$ ) with respect to the stretch rate at initial pressures of 1 and 2 bar across different equivalence ratios of (a) H<sub>2</sub>-O<sub>2</sub>-40% CO<sub>2</sub> and (b) H<sub>2</sub>-O<sub>2</sub>-60% CO<sub>2</sub>.

Figure 3(b) represents the flame speed versus stretch rate for the 60% CO<sub>2</sub> case at stoichiometric and lean conditions and initial pressures of 1 bar and 2 bar. It is evident from the plot that at both the atmospheric and elevated pressures, the stoichiometric conditions show the highest flame speed. At  $\phi = 0.8$ , the flame speed remains similar but once it drops to  $\phi = 0.6$ , the flame speed decreases drastically. Similar trends are observed at the elevated pressure of 2 bar, but at a lower magnitude. Furthermore, in all the cases tested in this study, higher stretch rates are measured at the early stages of flame propagation. As the flame propagates, the stretch rate reduces, resulting in an increase of flame speed [14-15]. By utilizing CO<sub>2</sub> as a working fluid, the high flame speeds of hydrogen oxycombustion can be reduced to match that of natural gas combustion in air. Figure 3(b) also shows that flame speeds measured from stoichiometric methane (CH<sub>4</sub>) combustion at 1 bar initial pressure coincides with that of hydrogen oxycombustion at  $\phi = 0.6$  and  $P_i = 2$  bar. The much steeper slope for hydrogen oxycombustion compared to that of CH<sub>4</sub> [11] will be discussed in the next section.

Figure 3(a) shows that the flame speed vs stretch rate curve for H<sub>2</sub>-O<sub>2</sub>-40% CO<sub>2</sub> carries a similar trend when compared to the 60% CO<sub>2</sub> data. The highest flame speeds are observed at stoichiometric conditions. The flame speed goes down as the conditions become leaner. Unlike the CH<sub>4</sub> and 60% CO<sub>2</sub> mixtures, where a decreasing flame speed trend is observed at higher pressures, the flame speed of H<sub>2</sub>-O<sub>2</sub>-40% CO<sub>2</sub> combustion tends to go up with the increasing initial pressure. This trend matches with the findings from Ijima and Takeno [12] for hydrogen-air combustion, which indicates that as the CO<sub>2</sub> percentage in the mixture starts to decrease, the data set begins to resemble the conditions

seen in standard hydrogen combustion. From the Schlieren images shown in Figures 1 and 2, it is quite evident that at higher pressures, instabilities start to appear quite early in the flame development. Since these self-accelerating cellular structures, commonly characterized by the Darrieus-Landau instability [16-17], become more dominant at higher pressures, the flame propagates at a much faster rate.

The data obtained from the flame speed versus stretch rate plots were utilized to calculate the burned gas Markstein length for the experiments conducted, as illustrated in Figure 4. An increasing trend in Markstein length is observed from stoichiometric to lean conditions when pressure is at 1 bar and CO<sub>2</sub> concentration is kept at 40%, but the opposite is observed for 60% CO<sub>2</sub> and 2 bars of initial pressure. As the CO<sub>2</sub> concentration is increased, the combustion characteristics start to mimic that of a methane combustion [11]. The initial pressure of the reactant mixture also has a significant effect on the Markstein length of hydrogen oxycombustion. Regardless of the mixture configuration (stoichiometric or lean) an increase in initial pressure results in a higher value of Markstein Length which can be attributed to increasing cellular instabilities initiating on the surface of the flame front at elevated pressures. This is due to the hydrodynamic instabilities at reduced laminar flame thicknesses [16] which results in an increased reacting surface area, corresponding to the rise in reaction rate and flame speed.

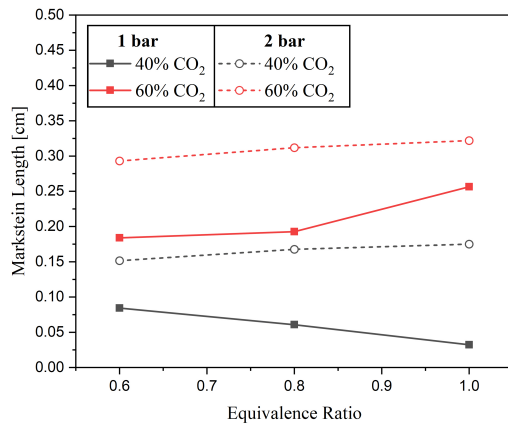


Figure 4: Markstein length against equivalence ratio for different initial pressures of H<sub>2</sub>-O<sub>2</sub>-CO<sub>2</sub> combustion.

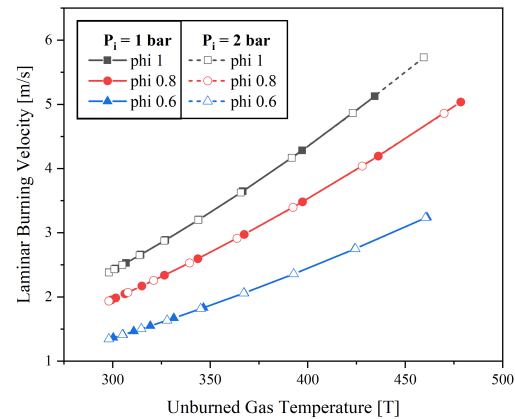


Figure 5: Effect of unburned gas temperature on the laminar burning velocity ( $S_u$ ) of premixed H<sub>2</sub>-O<sub>2</sub>-60% CO<sub>2</sub> combustion experiments.

### 3.3 Laminar Burning Velocity

For all the observed cases, a positive correlation between the measured laminar burning velocity ( $S_u$ ) and the unburned gas temperatures ( $T_u$ ) was observed for H<sub>2</sub>-O<sub>2</sub>-CO<sub>2</sub> combustion, which is illustrated in Figure 5. Furthermore, all the CO<sub>2</sub> concentrations and initial pressures had the highest laminar burning velocity at stoichiometric conditions and started to decrease in magnitude as the mixture became leaner. This can be attributed to an increasing trend of adiabatic flame temperature with increasing equivalence ratio from lean to stoichiometric conditions [18].

The magnitude of LBV was much closer to that of natural gas when hydrogen was burned at an equivalence ratio of  $\phi = 0.6$  with 60% CO<sub>2</sub>, which suggests the possibility of achieving flames like that of natural gas in air. At higher concentrations of CO<sub>2</sub>, the spherically propagating flames do not have as many cellular structures on its surface as it would be seen on a standard hydrogen-air combustion, which reduces the flame speed.

### 4. Conclusions

The effect of using CO<sub>2</sub> as a working fluid for oxycombustion of H<sub>2</sub> at different initial pressures and equivalence ratios in an optically accessible CVCC has been studied in terms of the flame structure, flame speed, Markstein length, and laminar burning velocity.

- In all the tested cases (different CO<sub>2</sub> concentrations and initial pressures), the highest flame speed and laminar burning velocity was achieved in stoichiometric conditions.
- Increasing the concentration of CO<sub>2</sub> in the mixture lowers the flame speed. In cases where the CO<sub>2</sub> concentration was increased to 60%, the measured flame speed and laminar burning velocity was seen to be similar to that of CH<sub>4</sub> combustion in air.
- At lower CO<sub>2</sub> concentrations (20% or 40%), the flame front propagated faster as the initial pressure was increased. The opposite trend was observed for 60% CO<sub>2</sub>, which resembles CH<sub>4</sub>-air combustion.

The inclusion of carbon dioxide as a working fluid in oxycombustion of hydrogen provides the opportunity to achieve flames with LBVs that are appropriate for practical combustion applications. It also eliminates the production of NO<sub>x</sub>

emissions and enables carbon separation or closed-cycle processes. Additional studies will be conducted to determine the parameters that enable the combustion of  $H_2$ - $O_2$ - $CO_2$  mixtures to approximate that of natural gas in air.

## 5. References

- [1] N.Abas, A.Kalair and N.Khan, "Review of fossil fuels and future energy technologies," *Futures*, vol. 69, pp. 31-49, 2015.
- [2] T. F. Stocker, D. Qin, G.-K. Plattner, M. Tignor, S. Allen, J. Boschung, A. Nauels, Y. Xia, V. Bex and P. M. (eds.), "'Climate Change 2013: The Physical Science Basis. Contribution of Working Group I to the Fifth Assessment Report of the Intergovernmental Panel on Climate Change," IPCC/Cambridge University Press, Cambridge, UK, 2013.
- [3] J. Kotcher, E. Maibach and W.-T. Choi, "Fossil fuels are harming our brains: identifying key messages about the health effects of air pollution from fossil fuels," *BMC Public Health*, vol. 19, p. 1079, 2019.
- [4] M. Wang, G. Wang, Z. Sun, Y. Zhang and D. Xua, "Review of renewable energy-based hydrogen production processes for sustainable energy innovation," *Global Energy Interconnection*, vol. 2, no. 5, pp. 436-443, 2019.
- [5] P. C. T. D. Boer, W. J. McLean and H. S. Homan, "Performance and emissions of hydrogen fueled internal combustion engines," *International Journal of Hydrogen Energy*, vol. 1, no. 2, pp. Pages 153-172, 1976.
- [6] S. Verhelst and T. Wallner, "Hydrogen-fueled internal combustion engines," *Progress in Energy and Combustion Science*, vol. 35, no. 6, pp. 490-527, 2009.
- [7] E. Bancalari, P. Chan and I. S. Diakunchak, "Advanced Hydrogen Gas Turbine Development Program," in *Turbo Expo: Power for Land, Sea, and Air*, Montreal, 2007.
- [8] W. Feng, L. Shibo, H. Yizhuo and J. Huiqiao, "The chemical effect of  $CO_2$  on the methane laminar flame speed in  $O_2/CO_2$  atmosphere," *IOP Conference Series: Earth and Environmental Science*, vol. 186, no. 2, 2018.
- [9] T. Cong and P. Dagaut, "Oxidation of  $H_2/CO_2$  mixtures and effect of hydrogen initial concentration on the combustion of  $CH_4$  and  $CH_4/CO_2$  mixtures: Experiments and modeling," *Proceedings of the Combustion Institute*, vol. 32, no. 1, pp. 427-435, 2009.
- [10] Y. S. Sanusi, E. M. A. Mokheimer, M. R. Shakeel, Z. Abubakar and M. A. Habib, "Oxy-Combustion of Hydrogen-Enriched Methane: Experimental Measurements and Analysis," *Energy Fuels*, vol. 31, no. 2, 2017.
- [11] M. Baghirzade, M. N. Nasim, B. Nawaz, J. Aguilar, M. Shahsavan, M. Morovatiyan and J. H. Mack, "Analysis of Premixed Laminar Combustion of Methane With Noble Gases as a Working Fluid," in *ASME 2021 Internal Combustion Engine Division Fall Technical Conference*, 2021.
- [12] T. Iijima and T. Takeno, "Effects of temperature and pressure on burning velocity," *Combustion and Flame*, vol. 65, no. 1, pp. 35-43, 1986.
- [13] F. Rahim, M. Elia, M. Ulinski and M. Metghalchi, "Burning velocity measurements of methane-oxygen-argon mixtures and an application to extend methane-air burning velocity measurements," *International Journal of Engine Research*, vol. 3, no. 2, pp. 81-92, 2002.
- [14] O. Kwon and G. Faeth, "Flame/stretch interactions of premixed hydrogen-fueled flames: measurements and predictions," *Combustion and Flame*, vol. 124, no. 4, pp. 590-610, 2001.
- [15] S.Kwon, L.-K.Tseng and G.M.Faeth, "Laminar burning velocities and transition to unstable flames in  $H_2/O_2/N_2$  and  $C_3H_8/O_2/N_2$  mixtures," *Combustion and Flame*, vol. 90, no. 3-4, pp. 230-246, 1992.
- [16] W. Kim, Y. Sato, T. Johzaki, T. Endo, D. Shimokuri and A. Miyoshi, "Experimental study on self-acceleration in expanding spherical hydrogen-air flames," *International Journal of Hydrogen Energy*, vol. 43, no. 27, pp. 12556-12564, 2018.
- [17] C.R.L.Bauwens, J.M.Bergthorson and S.B.Dorofeev, "Experimental investigation of spherical-flame acceleration in lean hydrogen-air mixtures," *International Journal of Hydrogen Energy*, vol. 42, no. 11, pp. 7691-7697, 2017.
- [18] M. Morovatiyan, M. Shahsavan, J. Aguilar, M. Baghirzade and J. H. Mack, "An Assessment of Hydrogen Addition to Methane Combustion with Argon as a Working Fluid in a Constant Volume Combustion Chamber," *Combustion Science and Technology*, 2021.